ARTICLE

Computational and Experimental Studies on Cu/Au-catalyzed Stereoselective Synthesis of 1,3-Disubstituted Allenes

Received 12 Mar 2019
Accepted 16 Apr 2019

DOI: 10.1039/C9QO00364A

María Magdalena Cid,*[a] María Lago-Silva,[a] Marta González Comesaña,[a] Olalla Nieto Faza[a] and Carlos Silva López *[a]

Cu- and Au-mediated formation of allenes from terminal alkynes and aldehydes via propargylamine intermediates is hampered by reversibility in the propargylamine formation. The use of a stable Au(I) catalyst in the reaction using a chiral propargylamine provided clues to disentangle the mechanism of the whole process that would have been otherwise hidden. Additionally, the process was observed to be stereoselective when an enantiomerically pure chiral propargylamine was used as starting substrate providing the corresponding 1,3-disubstituted allenes with high enantiomeric ratio.

Introduction

In the last decade, allenes have gained importance in organic chemistry due to their structural properties and reactivity.[1-3] They are also present in several biologically active natural compounds as well as in pharmaceuticals.[4] As a result, there is an ongoing interest in efficient synthetic routes to obtain allene substrates from simple and readily available starting materials. There are three main catalytic methods reported in the literature which directly provide the three carbon allene-core from the connection of two fragments: i) allene cross-metathesis, mainly used for symmetrically disubstituted allenes,[5] ii) masked-carbene/vinylidene cross-coupling between enamines and terminal alkynes mediated by a cationic Au(I) complex[6] and iii) the Crabbé homologation,[7,8] where an alkyne and formaldehyde react in the presence of CuBr, leading to the formation of a terminal allene as product via a Mannich base (propargylamine) intermediate **1**. This methodology features a stepwise reaction pathway with a retro-imino-ene rearrangement as the key step of the process (see Scheme 1a). We have shown that the main role of the copper catalyst is the activation of the alkyne moiety, and the stabilization of both the zwitterionic intermediate **3** and the incipient vinyl carbanion at the transition state **4**.[9] Unfortunately, although this reaction works really well with formaldehyde as a homologating agent, the preparation of di- and trisubstituted allenes suffers severe limitations using this methodology. A number of researchers have tried to overcome this limitation either replacing DIPA or CuBr by more reactive species. Thus, Ma succeeded in the one-pot synthesis of disubstituted allenes from 1-alkynes using morpholine and ZnI_2,[10,11] whose main role is to facilitate the [1,5]-hydride migration and the stabilization of the zwitterionic intermediate as it was concluded from the study of the reaction mechanism carried out by Zhang.[10,11] Mukai obtained disubstituted allenes performing the reaction under microwave irradiation conditions.[12] Ma has also reported successful approaches to this chemistry through exotic mixtures of catalysts, like $CuI/ZnBr_2/Ti(OEt)_4$, in which CuI and $Ti(OEt)_4$ cooperate in the formation of the propargyl amine and $ZnBr_2$ is responsible for the formation of the final allene.[13] A two-pot version of this reaction based on the sequential use of $ZnCl_2$ and $ZnBr_2$ to obtain the propargyl amine and the final allene, respectively, has also been developed by Periasamy.[14] In another approach, the intermediate propargylamines **1** were used as substrate in a metal mediated reaction (Pd, Ag, Au) to obtain the corresponding 1,3-disubstituted allenes.[15-18]

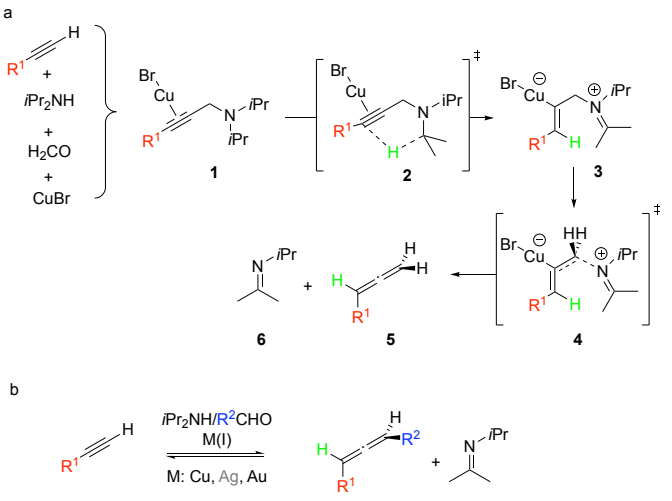

Scheme 1. a) Mechanism for the formation of terminal allenes from Mannich bases **1**; b) alkyne homologation reaction for the preparation of 1,3-disubstituted allenes.

[a] *Departamento de Química Orgánica, Universidade de Vigo, Campus Lagoas-Marcosende, 36310 Vigo (Spain)*

Electronic Supplementary Information (ESI) available: Experimental procedures, compound characterisation and computed geometries of all intermediates and transition states. See DOI: 10.1039/x0xx00000x

In particular, the palladium mediated asymmetrization of racemic allenes with simultaneous control of axial and center chirality in the final product has just been described by Ma.[19,20] Through allenylation of terminal alkynes, Ma and Zhang reported on the formation of disubstituted allenes via dimerization of terminal alkynes with CdI_2.[21,22] However, there is still a need for a more efficient and general protocol for the synthesis of polysubstituted allenes.

In this work, we aim at providing an alternative efficient methodology to add to the organic chemist toolbox to prepare chiral polysubstituted allenes. To do so, first we identified which are the main mechanistic features that hinder Crabbé conditions from forming disubstituted allenes by comparing the homologation reaction with formaldehyde and acetaldehyde. Additionally, we included the possibility of using softer and more alkynophilic metals (Ag and Au) as potential candidates to outperform the copper catalytic system (see Scheme 1b). The outcome of the computational study led us to prepare successfully chiral allenes with high *ee*.

Results and discussion

Computational study on the homologation with formaldehyde

First, we computed the Cu-catalyzed and non-catalyzed transformation of formaldehyde into terminal allenes by the concurrence of a secondary amine and a terminal alkyne to explore afterwards the behavior of silver (I) and gold (I) catalysts (energies were computed at the M06-2X/6-31+G(d,p)-LanLDZ level and 1,4-dioxane parameters for the PCM solvation model. See the methods section in the ESI for details). Since the Mannich base formation was supposedly not rate-limiting, **1** was chosen as the starting point of the mechanism.[$] Our results show that the use of AgBr as catalyst slightly improved the results obtained with copper catalysts (see orange and yellow lines in Figure 1) in less than 2 kcal/mol, a difference that is constant along the reaction pathway.

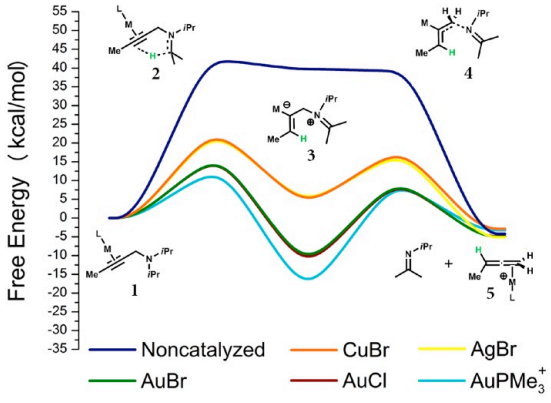

Figure 1. Profiles of the catalyzed and uncatalyzed reaction of formaldehyde-derived propargylamine **1** to allene **5**. (Relative free energies computed at the M06-2X/6-31+G(d,p)-LanLDZ level and 1,4-dioxane as implicit solvent)

Table 1: Relative SCF and Gibbs free energies (in kcal/mol) for the intermediates and transition states involved in the reaction profiles illustrated in Figure 1. Blue values indicate the rate-determining transition state for each reaction.

	Non-cat		CuBr		AgBr		AuBr		AuCl		$AuPMe_3$	
	SCF	Δ*G*	SCF	Δ*G*	SCF	Δ*G*	SCF	Δ*G*	SCF	Δ*G*	SCF	Δ*G*
1	0.0	0.0	0.0	0.0	0.0	0.0	0.0	0.0	0.0	0.0	0.0	0.0
2	41.2	40.7	20.6	20.6	19.1	18.7	16.4	16.4	16.8	16.9	10.0	10.3
3	39.8	39.9	0.9	2.9	-0.6	1.3	-10.4	-8.4	-10.5	-8.2	-22.2	-20.3
4	41.8	39.8	17.6	15.0	15.8	13.1	10.7	7.0	10.9	7.5	11.2	4.9
5	9.3	-6.7	12.3	-3.9	11.2	-5.6	9.9	-6.2	9.7	-6.3	14.0	-2.4

The energy requirements for the reaction further decreases when gold bromide was used (see green line in Figure 1 and energy data in Table 1) resulting in a significant improvement with respect to the parent system. Considering the ligand-differentiating effect on gold catalysts,[23,24] other non-expensive neutral and cationic Au(I) catalysts(AuCl and $AuPMe_3^+$) were explored.[‡] At first sight, the results show that varying the halide counterion on gold seems to have a negligible effect since the profiles of AuCl and AuBr are almost superimposable and that addition of a π-retrodonating ligand (i.e. PPh_3) does affect the overall mechanism lowering the first activation barrier by ca. 7 kcal/mol (blue line in Figure 1 and Table 1).

Interestingly a number of basic features are well conserved in all the computed reaction profiles: 1– The three metals significantly reduce the non-catalyzed barrier (to half its value or more); 2– The metal center significantly stabilizes the zwitterionic intermediate **3** in all catalyzed profiles; and 3– in all the metal halides the second transition state is less energetic (ca. 6 kcal/mol for CuBr and AgBr; and ca. 9 kcal/mol for gold halides) than the first one. However, while the initial hydride transfer (**2** in Figure 1) is the rate-limiting step for the uncatalyzed and the metal halide mediated reactions, the $AuPMe_3^+$ profile suggests that the formation of allene **5** via transition state **4** becomes now the rate-limiting step. Given these results, we decided to explore the nature of the Au(I)-activation further.

Role of the Gold ligand

Our data showed a clear difference in reactivity when changing neutral (AuCl and AuBr) for cationic complexes ($AuPMe_3^+$) as gold catalysts. Thus, in order to account for the difference in stabilization of the zwitterionic intermediate **3**, we considered the effects that the different ligands exert on the Au—C bond present in **3** using Natural bond orbital (NBO) analysis to calculate the charge transfer interactions.[§]

A NBO analysis[25,26] of intermediate **3** involving the cationic $AuPMe_3^+$ catalyst revealed a strong bidirectional charge delocalization between the C—Au and Au—P bonds. These electron delocalization patterns are illustrated in Figure 2 and have an associated energy of 61.9 kcal/mol for the $\sigma_{C-Au} \rightarrow \sigma^*_{Au-P}$ and 42.1 kcal/mol for the $\sigma_{Au-P} \rightarrow \sigma^*_{C-Au}$ with respect to the localized Lewis structure. The effect of this charge delocalization is also well reflected in the Au—C bond length. The electron donating PMe_3 results in a Au—C bond length slightly longer (from 2.019 Å in AuCl to 2.073 Å in $AuPMe_3^+$, see Table 2).

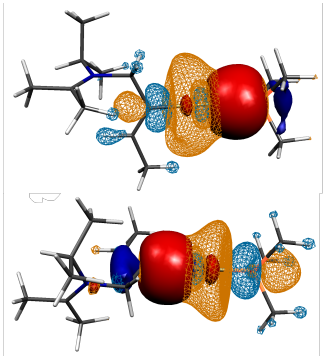

Figure 2. Representation of the orbitals in **3** to show the delocalization between C—Au and Au—P bonds in PMe_3Au^+: top, $\sigma_{Au-P} \rightarrow \sigma^*_{C-Au}$, and bottom, $\sigma_{C-Au} \rightarrow \sigma^*_{Au-P}$

Hence cooperative retrodonation between the activated substrate and the phosphine results in an increased stability of intermediate **3** due to electron delocalization. At the same time this retrodonation involves the participation of the Au—C antibonding orbitals, making this bond more labile. An AIM analysis[27,28] of intermediate **3** showed an increase in the electron density at the Metal—C bond critical point (ρ_{BCP}) when going from copper to gold (Table 2) suggesting that the Au—C bond has an enhanced covalent nature.

The Laplacian $\nabla^2\rho$ values at the BCP for the C—Metal bond in the entire series of ligands are always positive and indicate that the bond is mainly of "closed shell" ionic character. However, the gold-carbon and silver-carbon bonds have more partial covalent character, being consistent with the Wiberg bond indices[29] obtained from NBO analysis (Table 2).

Table 2: Topological properties of the electron density of **3** at the C—M bond critical point (BCP).

	CuBr	AgBr	AuCl	AuBr	$AuPMe_3$
$R_{C\text{-}M}$[a]	2.006	2.184	2.019	2.028	2.073
ρ_{BCP}[b]	0.013	0.086	0.137	0.134	0.123
$\nabla^2\rho_{BCP}$[c]	0.348	0.230	0.259	0.248	0.237
Bond order[d]	0.024	0.437	0.660	0.643	0.558

[a]Computed C—M bond distance. [b]Electron density at the bond critical point (BCP). [c]Laplacian of the electron density at the BCP. [d]Wiberg bond index.

Computational study on the homologation with acetaldehyde

Having computed that Au(I) (either in a neutral or cationic complex) would catalyzed the transformation of propargylamines **1** more efficiently than copper salts, we decided to explore the possibility of using α-substituted propargylamines to obtain 1,3-disubstituted allenes. To identify which of the steps of the homologation becomes unproductive when trying to produce disubstituted allenes, we also computed the reaction profiles with the CuBr and AgBr catalysts.[§§]

In this case however, due to the chiral center present at the propargylic position, the migration of the hydrogen from the DIPA moiety can follow two paths (path a or b, see Figure 3). As in the previous system, the reaction follows a stepwise mechanism in which two alternative hydrogen migrations are possible that are not equally probable since there is a considerable energy shift of ca. 8 kcal/mol that propagates along the entire process.

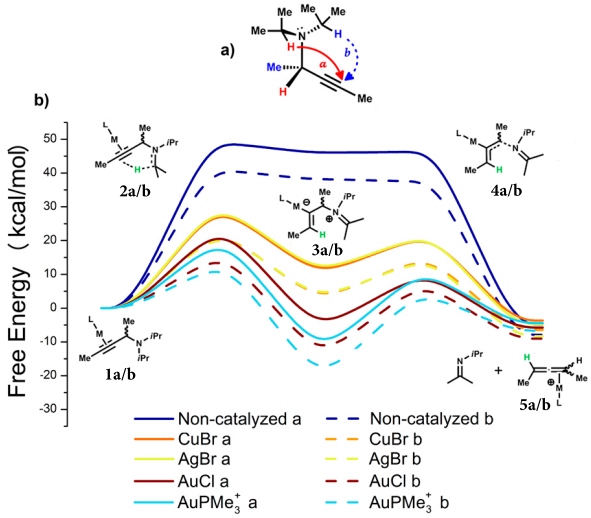

Figure 3. [1,5]-hydrogen migrations: a) pathway *a* (red) and *b* (blue); b) profiles for the non-catalyzed and metal-catalyzed reactions for the two alternate paths. (Relative free energies computed at the M06-2X/6-31+G(d,p)-LanLDZ level and 1,4-dioxane as implicit solvent)

The more favorable path involves the proton on the same side of the alkyl substituent (pathway b, see Table 3 and Figure 3), although this issue has no stereochemical consequences unless a scalemic mixture of propargylamines is employed.

The inclusion of CuBr in the mechanism reduces the activation barrier by ca. 20 kcal/mol and Ag(I) again slightly improves the copper results (Table 3 and Figure 3). Gold catalysts feature here also the highest catalytic capabilities: AuCl reduces the activation energy for the initial step, when compared with the Cu(I), in ca. 5 kcal/mol, and gold phosphine reduces even more this barrier (10 kcal/mol). However, the strong stabilization of intermediate **3a** results in a higher barrier for the formation of the allene (see Table 3 and light blue line in Figure 3b) and, as a consequence, the second step becomes rate-limiting.

Table 3: Relative SCF and Gibbs free energies (in kcal/mol) for the intermediates and transition states involved in the reaction profiles illustrated in Figure 3. Blue values indicate the rate-determining step for each reaction. The less favourable pathway *a* in faded hue.

	Non-cat		CuBr		AgBr		AuCl		$AuPMe_3$	
	SCF	Δ*G*	SCF	Δ*G*	SCF	SCF	Δ*G*	SCF	SCF	Δ*G*
1a/b	0.0	0.0	0.0	0.0	0.0	0.0	0.0	0.0	0.0	0.0
2a	47.0	47.4	26.2	26.9	24.7	25.9	22.6	23.7	15.9	17.0
2b	40.4	39.3	20.4	19.6	18.7	19.5	16.8	16.0	9.9	9.5
3a	45.8	46.5	7.1	9.7	6.6	8.6	-3.3	-0.9	-15.3	-12.4
3b	39.3	38.8	0.6	1.6	-0.7	0.4	-9.9	-8.8	-21.7	-21.1
4a	46.9	46.9	20.6	18.5	18.9	17.3	11.5	9.5	9.5	6.8
4b	40.0	38.2	14.9	12.1	12.9	10.1	9.2	6.3	4.3	0.6
5a	9.6	-6.9	12.1	-4.3	11.4	-4.8	9.3	-6.4	13.4	-3.6
5b	6.9	-9.9	9.5	-7.2	8.6	-8.8	7.0	-9.9	10.6	-6.2

A comparison of the energy profiles for both systems, furnishing mono-and disubstituted allenes, shown in Figure 1 and 3,

suggests that there is no significant energy penalty associated to the formation of disubstituted allenes, 20.6 vs 19.6 kcal/mol in the case of Cu(I) catalyst from either propargylamine **1**. From these data we derive that the formation of the initial Mannich base **1** must become a key step when disubstituted allenes are the target compound and substituted aldehydes are needed as the reactants for a one-pot Crabbé homologation process (see below).

Gold-catalyzed synthesis of disubstituted allenes

The computational exploration described above provided some intriguing results: 1– The copper catalyst should be as effective with acetaldehyde as it is with formaldehyde once the propargylamine (Mannich base) **1** is formed. Hence, the reason for the Crabbé homologation failing to yield disubstituted allenes should lie elsewhere in the mechanism; 2– The transformation of the propargylamine **1** into allenes is activated by gold catalysts better than copper salts; and 3– the trajectory of H-migrations computed in a chiral Mannich base **1** suggests that an enantioselective process could be envisioned to afford enantiopure 1,3-disubstituted allenes. In order to confirm the conclusions derived from our computational study, propargylamine **1-Ph,Ph** was prepared in 87% yield from commercially available reagents following the conditions reported by Knochel[30] (scheme 2).

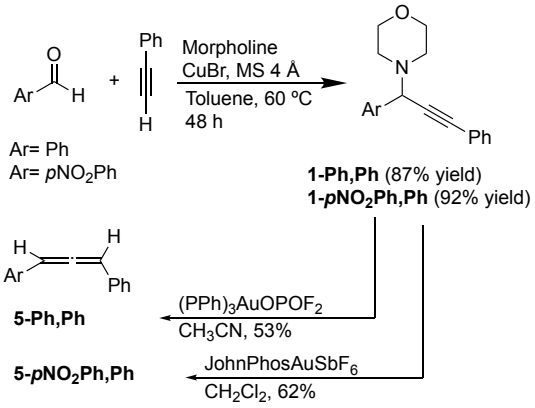

Scheme 2. Synthesis 1,3-disubstituted allenes **5** from α-substituted propargylamines **1**

Next, treatment of **1-Ph,Ph** with CuBr in 1,4-dioxane at 80 °C yielded traces of the corresponding allene **5-Ph,Ph** after 6 days as indicated by the appearance of the allene ^{1}H-NMR signal at 6.60 ppm and ^{13}C NMR signals at 98.2 and 207.5 ppm (see Figure S1 in the ESI). Higher temperatures had deleterious effects on the reaction yield. The formation of trace amounts of allene is in good agreement with the conclusions derived from computation. In fact, the prolonged reaction times when compared with the usual formaldehyde process also suggests that the Mannich base becomes a key factor when substituted aldehydes are used. The Au(I)-catalyzed reaction (AuCl or $(Ph_3P)AuSbF_6$) performed better but resulted in a low conversion rate and yield as a consequence of the fast decay of the gold catalysts to Au^0 species (detected by the appearance of colloidal gold/gold mirror), which are less active or non-reactive gold states.[31,32] In order to minimize the disproportionation process, we changed the solvent to acetonitrile and the counterion of the gold phosphine from SbF_6^- to $OPOF_2^-$.[33] Thus, allene **5** was obtained in 53% yield with total conversion of the Mannich base **1-Ph,Ph** when $(Ph_3P)AuOPOF_2$ in CH_3CN was used at room temperature in 6 days. Intriguingly, small amounts of benzaldehyde were detected by NMR in the reaction mixture.

In order to confirm the center-to-axis chirality transfer[34,35] from propargylamines into allenic products, chiral propargylamine **1-Ph,Ph** was prepared in 63% yield (60% ee) via A^3-coupling of benzaldehyde, phenylethyne and morfoline in the presence of CuBr using (*R*)-(+)-QUINAP as chiral inducer (scheme 3).[36,37] Reaction of the resulting propargylamines (-)-**1-Ph,Ph** or (+)-**1-Ph,Ph** with $(PPh_3)AuOPOF_2$ in acetonitrile at room temperature rendered diphenylallene **5** with a modest enantiomeric excesses (~15% ee). The absolute configuration of allene **5-Ph,Ph** was assigned by comparison of the HPLC trace and circular dichroism (CD) spectra (Figure 4) with the reported ones.[38,39]

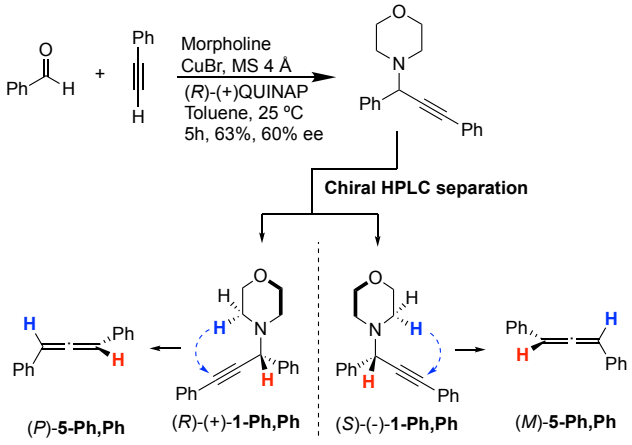

Scheme 3. Preparation of enantiopure propargylamines **1-Ph,Ph**. HPLC (Chiralpak IA, hexane/AcOEt (2%), 1.6 mL/min): t_R(min)= 22, (-)-**1-Ph,Ph**; 27, (+)-**1-Ph,Ph.**

When (-)-**1-Ph,Ph** was used, the obtained allene **5-Ph,Ph** showed a negative Cotton effect at 255 nm and a positive one at 232 nm in the ECD spectrum that compares well with the reported spectrum for pure allene (*M*)-**5-Ph,Ph** (red line in Figure 4). Similarly, reaction with (+)-**1-Ph,Ph** provided allene (*P*)-**5-Ph,Ph**, whose ECD spectrum was, as expected, a mirror image of the ECD spectrum of its enantiomer (blue line in Figure 4). However, the fact that the reaction enantioselectivity was modest made us to consider whether side reactions were competing with the allene formation. To do so, we considered two scenarios: 1- Isomerization processes either before or after allene formation; 2- Reversibility in the formation of the Mannich base under the reaction conditions.

Regarding isomerization events, if intermediate **3** was sufficiently long-lived, a C—C bond rotation could poise the structure ready for the cleavage of the imine moiety in syn position with respect to the M—C bond, leading to the enantiomeric allene and, as a consequence the selectivity of the reaction would be lower.

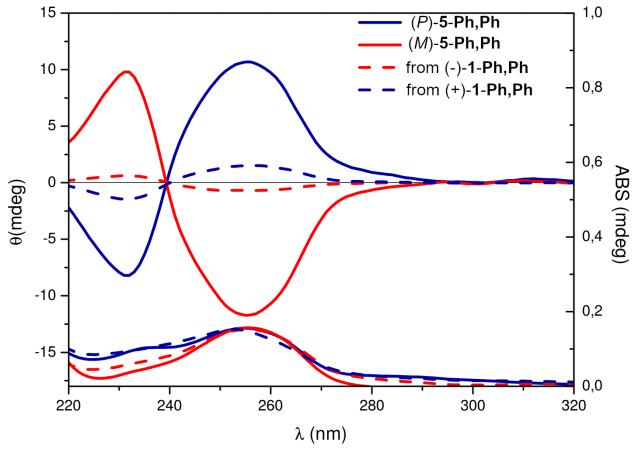

Figure 4. Absorbance (bottom) and CD (top) spectra of pure (*M*)- (solid red) and (*P*)-**5-Ph,Ph** (solid blue) in hexane at ca. 10^{-4} M; and of the crude reaction mixture of (-)-**1-Ph,Ph** (dash red) and (+)-**1-Ph,Ph** (dash blue) as starting substrates.

However, the computed barrier for the cleavage of such intermediate is higher in 13 and 8 kcal/mol than the corresponding anti cleavage for the reactions with formaldehyde- and acetaldehyde-derived propargylamines **1**, respectively, rendering these processes non-competitive (see Figure S23 in the ESI). On the other hand, allene isomerization could also be a way of losing stereoselectivity. However, when a sample of pure allene (*P*)-**5-Ph,Ph** was submitted to the reaction conditions ($(PPh_3)AuOPOF_2$ in acetonitrile at room temperature) for two weeks its CD signal barely decreased (see Figure S3a). On the contrary, the g-factor, defined as the ratio between the ECD and absorbance signals, was drastically reduced in a time span of three days when the sample was left on the lab bench exposed to ambient light (see Figure S3b). Nonetheless, none of these results are compatible with the reduced enantioselectivity observed in the reaction since they are: 1-too slow compared with the reaction times employed and 2-our reactions were carefully carried out in the darkness.

Since the ^{1}H NMR spectra of the crude reaction mixtures featured small amounts of benzaldehyde, a reversible formation of **1** via a competitive retro-Mannich reaction occurring concomitantly with the allene formation seemed a plausible cause for the moderate stereoselectivity. This process would provoke partial racemization of **1** and prolonged reaction times due to the effective reduction of concentration of the propargylamine. A closer look into the mechanism of the reaction revealed that whereas theoretical reaction Gibbs free energies for the Mannich base formation with benzaldehyde is -5.9 kcal/mol, with formaldehyde it becomes -17.5 kcal/mol. This difference in the relative stability of reagents and products could explain why the reaction with formaldehyde led to the final allene product while, with benzaldehyde, an equilibrium between the retro-Mannich and the hydride transfer reaction is stablished. Therefore, the driving force for the successful formaldehyde reaction is its inherent instability, and any other aldehyde will suffer reversion of the propargylamine intermediate **1** to reactants.

Following this idea, the calculated data of thermodynamic stabilities of different aldehydes versus the corresponding Mannich bases (see Figure S22) led us to consider *p*-nitrobenzaldehyde (ΔG_R is twice that of benzaldehyde) as a good option to study the stereoselective pathway to prepare allene **5-*p*NO$_2$Ph,Ph**. Dichloro- or trichloroacetaldehyde were found to be more favourable (up to ~15 kcal/mol) but the ability of the trichloromethane group to act as a leaving group or the presence of α-H to render enamides, respectively, prevented their usage.

Thus, *p*-nitrobenzaldehyde was submitted to Knochel's conditions and after two days, the reaction rendered the Mannich base **1-*p*NO$_2$Ph,Ph** in 92% yield. The reaction of propargylamine **1-*p*NO$_2$Ph,Ph** under catalysis of $(PPh_3)AuOPOF_2$ in CH_3CN rendered allene **5-*p*NO$_2$Ph,Ph** in 50% yield (^{1}H NMR estimated) and in 62% (after column chromatography) when the reaction was carried out with JohnPhosAuSbF$_6$ in DCM (scheme 2). In both cases there were no traces of the aldehyde reactant, suggesting that the thermodynamic stability of *p*-nitrobenzaldehyde locks the retro-Mannich process. When enantiopure propargylamine (-)-**1-*p*NO$_2$Ph,Ph** was treated with JohnPhosAuSbF$_6$ in dichloromethane at room temperature, enantiopure allene (-)-**5-*p*NO$_2$Ph,Ph** was obtained in 90% ee (Scheme 4). Unsurprisingly the (+)-enantiomer yielded similar results (See ESI for the details).

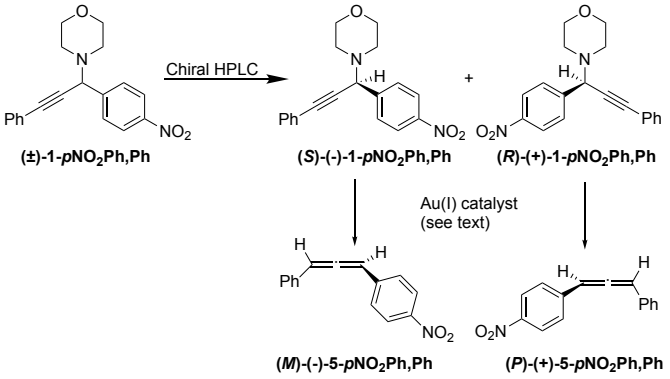

Scheme 4. Enantioselective synthesis of allenes **5**

Following Lowe-Brewster[40,41] rule to determine the absolute configurations of substituted allenes, the less polar (-)-**5-*p*NO$_2$Ph,Ph** presents an absolute configuration (*M)* or (*aR)*. The circular dichroism spectra of both enantiomers are mirror images and there is a good correlation between the experimental and TDDFT calculated CD spectra for the (*M*)-(-)-**5-*p*NO$_2$Ph,Ph** (Figure 5).

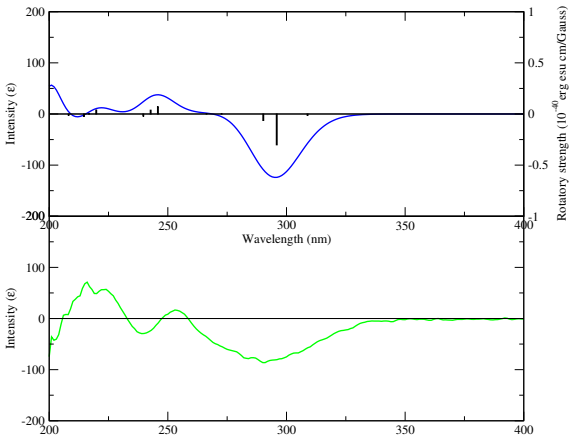

Figure 5. Theoretical (top) and experimental (bottom) ECD spectrum. The intensity of the latter has been adjusted arbitrarily

Thus, taking into account the results for **1-Ph,Ph** we assigned the configuration (*S)* to (-)-**1-*p*NO_2Ph,Ph**.

Conclusions

In summary, a retro-imino-ene process operates in the [1,5]-H migration reaction of propargylamines mediated by Cu(I), Ag(I) and Au(I) to yield allenes. The similarity of the reaction profiles for formaldehyde- and acetaldehyde-derived propargylamines suggests that the propargylamine formation is a key step on the unproductive formation of 1,3-disubstituted allenes with Cu(I) in the one-pot Crabbé homologation reaction of terminal alkynes with aldehydes. This is confirmed experimentally with the observation of aldehyde signals due to the Mannich base reverting to its forming products. In both reactions (formaldehyde/acetaldehyde) gold is computationally found to be a good candidate for the catalytic formation of disubstituted allenes. In the gold phosphine-mediated reaction the strong stabilization of intermediate **3** due to retrodonation interactions results in the final allene formation step becoming rate limiting. The Au-catalyzed hydrogen-migration reaction provides better results when a stability enhanced gold catalyst (JohnPhosAuSbF_6 or PPh_3AuOPOF_2) was used. In agreement with the theoretical results, the use of chiral propargylamines provided an enantioselective reaction. The modest values of enantioselection have been traced back to the reversibility of the Mannich base formation. The reaction driving force is the relative instability of the starting formaldehyde and this is the main cause for the reaction failing to provide disubstituted allenes. The use of *p*-nitrobenzaldehyde provided 1,3-disubstituted allenes with high ee, by circumventing the competitive retro-Mannich reaction.

Conflicts of interest

There are no conflicts to declare.

Acknowledgements

Financial support from Ministerio de Economia y Competitividad of Spain (CTQ2016-75023-C2-2-P and CTQ2017-85919-R), Xunta de Galicia (ED431C 2017/70) is gratefully acknowledged. The authors thank Dr. Fernando López and Prof. Antonio Echavarren for helpful discussions.

Notes and references

$ The mechanistic study reported by Fillion et al. (ref. 7) showed that the propargylamine or Mannich base can be isolated to later be subjected to a retro-ene-like reaction. Thus, its formation is hence proven experimentally to be not the rate-determining step.

‡ In the latter the counterion effect was not considered explicitly since, unlike in the gold halides, dissociation is expected under the reaction conditions, since the phosphine ligand is bonded to gold across the entire process.

§ The energetic importance of these interactions between filled donor and empty acceptor NBOs are estimated by second-order perturbation theory

§§ AuBr was not included here since both gold halides provided essentially the same catalytic activity for terminal allenes.

1 F. Inagaki, S. Kitagaki and C. Mukai, *Synlett*, 2011, **2011**, 594–614.
2 P. Rivera-Fuentes and F. Diederich, *Angew. Chem. Int. Ed.*, 2012, **51**, 2818–2828.
3 A. Hoffmann-Roder and N. Krause, *Angew. Chem. Int. Ed.*, 2004, **43**, 1196–1216.
4 S. Míguez-Lago and M. M. Cid, *Synthesis* 2017, **49**, 4111-4123.
5 M. Ahmed, T. Arnauld, A. G. M. Barrett, D. C. Braddock, K. Flack and P. A. Procopiou, *Org. Lett.*, 2000, **2**, 551–553.
6 V. Lavallo, G. D. Frey, S. Kousar, B. Donnadieu and G. Bertrand, *Proc Natl Acad Sci U S A*, 2007, **104**, 13569–13573.
7 P. Crabbé, H. Fillion, D. André and J.-L. Luche, *J. Chem. Soc., Chem. Commun.*, 1979, 859–860.
8 H. Fillion, D. André and J.-L. Luche, *Tetrahedron Lett.*, 1980, **21**, 929–930.
9 M. González, R. Álvarez Rodríguez, M. M. Cid and C. S. López, *J. Comput. Chem.*, 2012, **33**, 1236–1239.
10 J. Kuang and S. Ma, *J. Am. Chem. Soc.*, 2010, **132**, 1786–1787.
11 X. Zhang, *Asian J. Org. Chem.*, 2014, **3**, 309–313.
12 S. Kitagaki, M. Komizu and C. Mukai, *Synlett*, 2011, **8**, 1129–1132.
13 Q. Liu, X. Tang, Y. Cai and S. Ma, *Org. Lett.*, 2017, **19**, 5174–5177.
14 M. Periasamy, A. Edukondalu and E. Ramesh, *ChemistrySelect*, 2017, **2**, 3937–3942.
15 H. Nakamura, M. Ishikura, T. Sugiishi, T. Kamakura and J.-F. C. O. Biellmann, *Org. Biomol. Chem.*, 2008, **6**, 1471–1477.
16 V. K.-Y. Lo, M.-K. Wong and C.-M. Che, *Org. Lett.*, 2008, **10**, 517–519.
17 V. K.-Y. Lo, C.-Y. Zhou, M.-K. Wong and C.-M. Che, *Chem. Commun.*, 2010, **46**, 213–215.
18 K. K. Y. Kung, V. K.-Y. Lo, H. M. Ko, G. L. Li, P. Y. Chan, K. C. Leung, Z. Zhou, M. Z. Wang, C.-M. Che and M.-K. Wong, *Adv. Synth. Catal.*, 2013, **355**, 2055–2070.
19 X. Tang, Y. Han and S. Ma, *Org. Lett.*, 2015, **17**, 1176–1179.
20 Y. Han and X. Zhang, *Asian J. Org. Chem.*, 2017, **6**, 1778–1782.
21 J. Dai, X. Duan, J. Zhou, C. Fu and S. Ma, *Chinese J. Chem.*, 2018, **36**, 387–391.
22 S. Song, J. Zhou, C. Fu and S. Ma, *Nature Communications*, 2019, **10**, 507.
23 D. Leboeuf, M. Gaydou, Y. Wang and A. M. Echavarren, *Org. Chem. Front.*, 2014, **1**, 759–764.

24 M. D. Levin and F. D. Toste, *Angew. Chem. Int. Ed. Engl.*, 2014, **53**, 6211–6215.
25 X. Li, *J. Comput. Chem.*, 2014, **35**, 923–931.
26 C. K. Kim, K. A. Lee, C. K. Kim, B.-S. Lee and H. W. Lee, *Chem. Phys. Lett.*, 2004, **391**, 321–324.
27 R. F. W. Bader, Atoms in Molecules: A Quantum Theory, Clarendon Press (Oxford University Press), 1994.
28 O. N. Faza and C. S. López, *J. Org. Chem.*, 2013, **78**, 4929–4939.
29 K. B. Wiberg, *Tetrahedron*, 1968, **24**, 1083–1096.
30 N. Gommermann, C. Koradin, K. Polborn and P. Knochel, *Angew. Chem. Int. Ed.*, 2003, **42**, 5763–5766.
31 A. Vogler and H. Kunkely, *Coordination Chemistry Reviews*, 2001, **219 - 221**, 489–507.
32 J. Oliver-Meseguer, J. R. Cabrero-Antonino, I. Domínguez, A. Leyva-Pérez and A. Corma, *Science*, 2012, **338**, 1452–1455.
33 M. Kumar, J. Jasinski, G. B. Hammond and B. Xu, *Chem. Eur. J.*, 2014, **20**, 3113–3119.
34 O. N. Faza, C. S. López and A. R. de Lera, *J. Org. Chem.*, 2011, **76**, 3791–3796.
35 N. T. Patil, *Chem. Asian J.*, 2012, **7**, 2186–2194.
36 N. Gommermann and P. Knochel, *Tetrahedron*, 2005, **61**, 11418–11426.
37 C. Zhao and D. Seidel, *J. Am. Chem. Soc.*, 2015, **137**, 4650–4653.
38 S. F. Mason and G. W. Vane, *Tetrahedron Lett.*, 1965, **6**, 1593–1597.
39 M. Periasamy, P. O. Reddy and N. Sanjeevakumar, *Eur. J. Org. Chem.*, 2013, **2013**, 3866–3875.
40 G. Lowe, *Chem. Comm.*, 1965, **0**, 411–413.
41 J. H. Brewster, in Topics in Stereochemistry, John Wiley & Sons, Inc., Hoboken, NJ, USA, 2007, vol. 2, pp. 1–72.